

Characterization of the diffraction spectra of one-dimensional k -component Fibonacci structures

R. W. Peng, Mu Wang, An Hu, S. S. Jiang, G. J. Jin, and Duan Feng

National Laboratory of Solid State Microstructures, Nanjing University, Nanjing 210093, China
and Center for Advanced Studies in Science and Technology of Microstructures, Nanjing 210093, China

(Received 21 April 1995)

We study in this paper the diffraction spectrum (Fourier transform) of a one-dimensional k -component Fibonacci structure (KCFS), which contains k different intervals and can be generated by a substitution rule. Theoretical and numerical calculations based on the geometrical models for atomic KCFS have been made. The structures with $1 < k \leq 5$ are quasiperiodic, and their Fourier transforms are the sum of weighted δ functions. These diffraction peaks can be indexed by a finite set of base vectors. The structures with $k > 5$, however, do not possess the Pisot property, and the diffraction spectra consist of neither Bragg peaks, nor diffuse scattering. They are singularly continuous instead. Multifractal analysis is employed to characterize the diffraction spectra in the case of $k > 5$. It is shown that the diffraction spectra present scaling properties around the values of wave vector. Moreover, a dimensional spectrum of singularities associated with the diffraction spectrum, $f(\alpha)$, demonstrates a genuine multifractality. We conclude that the one-dimensional k -component Fibonacci structures provide a generic structural model covering periodicity ($k=1$), quasiperiodicity ($1 < k \leq 5$), and multifractality between quasiperiodicity and disorder ($k > 5$).

I. INTRODUCTION

In recent years much attention has been paid to one-dimensional (1D) ordered distributions, especially to the quasiperiodic systems.¹⁻⁶ Most studies are motivated by the discovery of quasicrystals.⁷ In theory, investigations on the nature of ground states of complex incommensurate structures are stimulating. The interest partly stems from the fact that quasicrystals are perfectly ordered, the Bloch theorem is inapplicable since there is no translational symmetry. In some sense, this problem represents an intermediate case between periodic and disordered solids. Parallel to the theoretical development in the field of quasicrystals, advances in experimental techniques have made it easy to produce artificial superlattices. Superlattice provides an excellent system to realize 1D quasiperiodicity. Usually the sample is quasiperiodic in the grown direction (z) and periodic in the xy planes. In 1985, Merlin *et al.*⁵ reported the realization of Fibonacci GaAs-AlAs superlattices. The Fibonacci sequence starts from A and reproduces according to the substitution rules $A \rightarrow AB$ and $B \rightarrow A$, in which the ratio of the two incommensurate intervals A and B is equal to the golden mean $\tau = (\sqrt{5} + 1)/2$. Several experiments^{6,8-10} on aperiodic superlattices have been reported since 1985. Yet very few studies have been performed so far on the 1D aperiodic structures with more than two incommensurate intervals.¹¹

In this paper, we present a theoretical investigation on the diffraction properties of 1D k -component Fibonacci structures (KCFS) created by the substitution rule $A_1 \rightarrow A_1 A_k$, $A_k \rightarrow A_{k-1}$, ..., $A_i \rightarrow A_{i-1}$, ..., $A_3 \rightarrow A_2$. The projection method is used to deal with the diffraction behavior of the KCFS with $k \leq 5$, and multifractal analysis is applied to characterize the Fourier spectra of the KCFS with $k > 5$. It is known that multifractal analysis is a suitable statistical description for the study of long term dynamical behavior of a physical system. For example, the invariant probability dis-

tribution on a strange attractor¹² and the spatial distribution of dissipative regions in a turbulent flow¹³ can be characterized by multifractal measures. The multifractal formalism relies on the fact that the highly nonuniform probability distributions arise from the nonuniformity of the system. Our investigations demonstrate that the diffraction spectra of the KCFS with $k > 5$ are highly nonuniform intensity distributions which possess scaling properties of multifractal.

II. PROPERTIES OF THE KCFS IN REAL SPACE

Let us begin with a few definitions of what we called k -component Fibonacci structures (KCFS). Consider the substitution T acting on an alphabet of k letters $A_1, A_2, \dots, A_i, \dots, A_k$, according to the rules

$$T \begin{cases} A_1 & \rightarrow A_1 A_k, \\ A_k & \rightarrow A_{k-1}, \\ \dots, \\ A_i & \rightarrow A_{i-1}, \\ \dots, \\ A_2 & \rightarrow A_1. \end{cases} \quad (1)$$

This substitution T is associated with a matrix M . Each line of M gives the numbers of letters $A_1, A_2, \dots, A_i, \dots, A_k$ which appear in the transforms of $T(A_1), T(A_2), \dots, T(A_i), \dots, T(A_k)$, respectively. Therefore this matrix can be expressed as

$$M = \begin{bmatrix} 1 & 0 & 0 & \dots & 1 \\ 1 & 0 & 0 & \dots & 0 \\ 0 & 1 & 0 & \dots & 0 \\ \vdots & \ddots & \ddots & \ddots & \vdots \\ \vdots & & \ddots & \ddots & \vdots \\ 0 & 0 & \dots & 0 & 1 & 0 \end{bmatrix}_{k \times k} \quad (2)$$

TABLE I. Parameters used in the calculations of the diffraction spectra from k -component Fibonacci structures (KCFS). n is the generation in the KCFS; $N_n^{(k)}=N$ is the total number of the atoms in the geometrical model of the KCFS.

Parameter \ Type	$k=2$	$k=3$	$k=4$	$k=5$	$k=6$	$k=7$	$k=8$	$k=9$	$k=10$	$k=20$	$k=30$	$k=40$	$k=50$	$k=80$	$k=100$
n	22	27	32	36	40	44	47	51	54	84	110	134	154	212	250
$N_n^{(k)}$	28657	27201	31422	29244	29548	31200	27428	30624	28711	31261	31410	32560	31760	32284	32250

Then the characteristic polynomial of matrix M is $P_k(\lambda) = \lambda^k - \lambda^{k-1} - 1$. It has been proved that for $1 < k \leq 5$ the substitution T possesses the Pisot property.¹⁴ This statement means that in all eigenvalues of matrix M there is only one eigenvalue λ_0 with its absolute value greater than 1.¹⁵ For $k > 5$, there is not any Pisot number in all eigenvalues of M . This feature is related to the structural tilings. The Bombieri-Taylor theorem¹⁶ provides a sufficient condition for the absence of quasiperiodicity: if there is a Pisot number in eigenvalues of the substitution matrix, the tiling is quasiperiodic and hence can be generated by a cut-and-projection method. Otherwise, the tiling is not quasiperiodic. Back to our case, the KCFS with $1 < k \leq 5$ are quasiperiodic, while the KCFS with $k > 5$ are nonquasiperiodic.

On the other hand, the KCFS can be described as a limit of the generation of the sequence $C_n^{(k)}$. Let $C_n^{(k)} = T^n A_1$. Thus

$$C_0^{(k)} = A_1,$$

$$C_1^{(k)} = A_1 A_k,$$

$$C_2^{(k)} = A_1 A_k A_{k-1},$$

$$\dots,$$

$$C_{k-1}^{(k)} = A_1 A_k A_{k-1} \dots A_3 A_2,$$

and in general $C_n^{(k)} = C_{n-1}^{(k)} + C_{n-k}^{(k)}$. Let $N_n^{(k)}(A_i)$ denote the number of A_i ($i=1, 2, \dots, k$) in $C_n^{(k)}$. The ratios of these numbers are defined as $\eta_i = \lim_{n \rightarrow \infty} [N_n^{(k)}(A_i) / N_n^{(k)}(A_1)]$. The set $\{\eta_i\}$ satisfies the following equations:

$$\eta_k^k + \eta_k = 1,$$

$$1 : \eta_k = \eta_k : \eta_{k-1} = \dots = \eta_i : \eta_{i-1} = \dots = \eta_3 : \eta_2. \quad (3)$$

It is easy to prove that all these ratios $\eta_i = \eta_k^{k-i+1}$ ($1 < i \leq k$) are irrational numbers between zero and unity except $\eta_1 = 1$; and η_k is just the reciprocal of the leading eigenvalue λ_0 of matrix M , $\eta_k = 1/\lambda_0$.

III. DIFFRACTION SPECTRA

The structural information can be demonstrated more clearly in reciprocal space. Studies on the diffraction spectra of the KCFS are based on a geometrical model of atom line. A one-dimensional geometrical structure is generated by putting atoms on a line. Each pair of the neighboring atoms is separated by a bond length which varies according to the sequence of letters. Here, the model of the KCFS with letters $A_1, A_2, \dots, A_i, \dots, A_k$ is associated with k real numbers, i.e., the bond lengths $l_{A_1}, l_{A_2}, \dots, l_{A_i}, \dots, l_{A_k}$. In order to avoid disappearance of some atoms in the long run and

eludes a lot of arbitrariness in the model, $\{l_{A_i}\}$ can be expressed by

$$l_{A_i} = \eta_i. \quad (4)$$

The Fourier transformation of this structure is performed in the following way. Firstly, the atomic density can be written as

$$\rho(z) = \sum_j \delta(z - z_j), \quad (5)$$

where z_j is the position of the j th atom on the line ($z_j - z_{j-1} = l_{A_1}$, or l_{A_2} , \dots , or l_{A_k} ; $z_0 = 0$). By denoting $F_n^{(k)}$ the Fourier amplitude of the above structure which contains the generation $C_n^{(k)}$ in the k -component Fibonacci (KCF) lattice, we have

$$F_n^{(k)}(Q) = \sum_{j=1}^{N_n^{(k)}} e^{-iQz_j}, \quad (6)$$

where $N_n^{(k)}$ is the number of letters in the generation $C_n^{(k)}$ (actually, it is also the number of atoms, or in other words, the sample size), and Q is the wave vector. The diffraction intensities associated with these amplitudes can be expressed as

$$I_n^{(k)}(Q) = \frac{1}{N_n^{(k)}} |F_n^{(k)}(Q)|^2. \quad (7)$$

Based on Eq. (7), diffraction spectra of the KCFS can be calculated. The generations (n) and the total number of atoms ($N_n^{(k)}$) in each sample are listed in Table I.

Figure 1(a) shows the diffraction spectra of a three-component Fibonacci (3CF) superlattice in one Brillouin zone (i.e., one period in reciprocal space). The Fourier transform of 3CF superlattice is a sum of weighted δ functions. From our discussions in Sec. II, η_3 for the 3CFS is a Pisot number. Therefore the 3CFS is quasiperiodic and can be generated by projection method. By projecting a cubic lattice with unit spacing along a line, a 3CF lattice in real space can be achieved. The Fourier transformation of this lattice indicates that the diffraction vectors have the following analytical form:¹¹

$$Q(n_1, n_2, n_3) = \frac{2\pi}{\bar{D}} \sum_{i=1}^3 n_i \eta_i,$$

$$\bar{D} = \sum_{i=1}^3 l_{A_i} \cdot \eta_i, \quad (8)$$

where n_i ($i=1,2,3$) are integers and \bar{D} is the average lattice wavelength. It is noteworthy that the strongest peaks reflect the self-similarity of reciprocal lattices, that is,

$$Q(a_{n+3}, a_{n+1}, a_{n+2}) = Q(a_{n+2}, a_n, a_{n+1}) + Q(a_n, a_{n-2}, a_{n-1}), \quad (9)$$

where a_n is defined as $a_n = a_{n-1} + a_{n-3}$ with $a_1 = a_2 = 0$ and $a_3 = 1$. Back to the numerical calculation of the 3CFS, one can easily find that the strong diffraction peaks illustrated in Fig. 1(a) can be indexed by three integers $[n_1, n_2, n_3]$ [shown in Fig. 1(a)], and the self-similarity is also satisfied, for example, $Q(1,1,1) = Q(1,0,1) + Q(1,0,0)$.

In fact, Fig. 1(a) is a typical diffraction spectrum of a quasiperiodic structure. According to Sec. II, the KCFS with $1 < k \leq 5$ are quasiperiodic. A low-dimensional quasiperiodic structure may be considered as the projection of high-dimensional periodic structure.¹⁷ Similarly, using the projection method (see Ref. 14 for details), we can obtain the following diffraction vectors:

$$Q(n_1, n_2, \dots, n_k) = \frac{2\pi}{\bar{D}} \sum_{i=1}^k n_i \eta_i,$$

$$\bar{D} = \sum_{i=1}^k l_{A_i} \cdot \eta_i, \quad (10)$$

where $1 < k \leq 5$. The diffraction spectra from the KCFS with $1 < k \leq 5$ contain Bragg peaks, each strong diffraction peaks can be indexed by k integers (n_1, n_2, \dots, n_k) . The self-similarity of the structure is displayed by the *locus* of the diffraction peaks.

The KCFS with $k > 5$ do not possess the quasiperiodicity. As k increases, the diffraction spectra of the KCFS become more and more complicated. Figures 1(b) and 1(c) show the diffraction spectra of six-component Fibonacci (6CF) and 100-component Fibonacci (100CF) structures, respectively. Comparing these two plots with Fig. 1(a), one may find that although discrete diffraction peaks can be found in Fig. 1(b), they cannot be indexed by integers. Consequently, self-similarity disappears from these spectra. As a result of increase of k , the diffraction spectra become more complicated. The diffraction spectrum shown in Fig. 1(c) is neither discrete nor continuous. Actually, it is singular continuous. These complicated diffraction spectra can only be described by statistical method up to now, and multifractal analysis would be a suitable candidate.

IV. MULTIFRACTAL ANALYSIS IN RECIPROCAL SPACE

Multifractal analysis is a tool for characterizing the nature of a positive measure in a statistical sense.^{18–21} By definition, a positive measure describes how a positive quantity is distributed on a set which is the support of the measure. If the

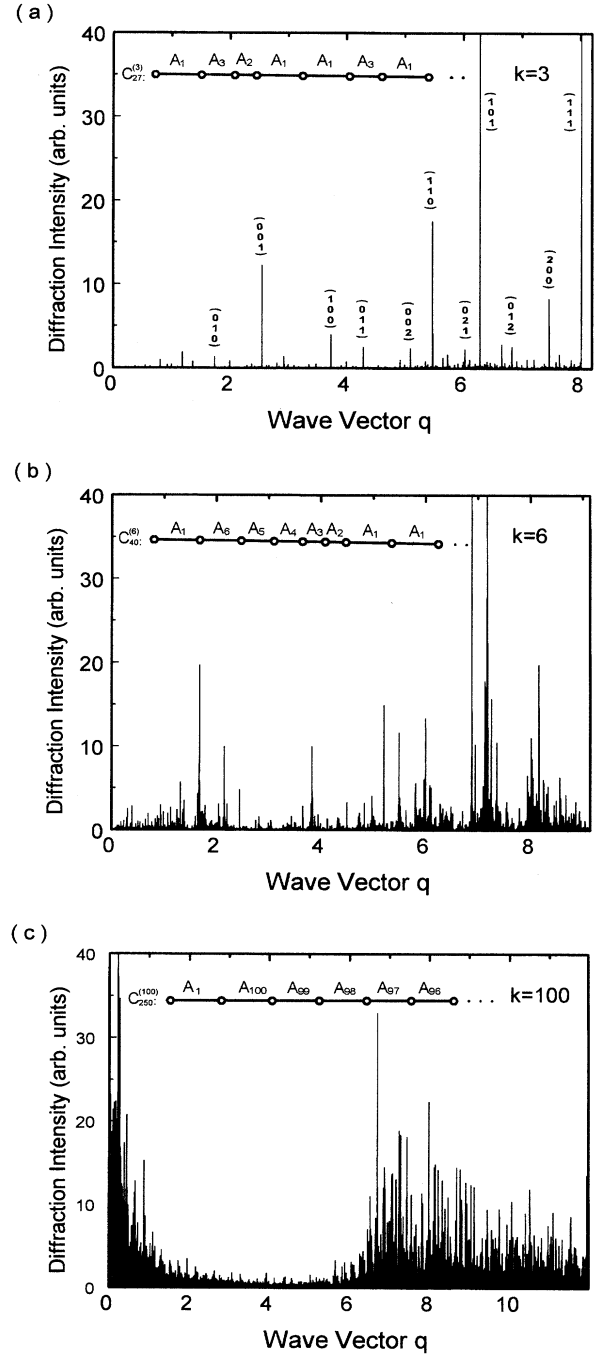


FIG. 1. The Fourier transforms of k -component Fibonacci (KCF) structures. The parameters for calculation are listed in Table I. (a) $k=3$. The 3CF geometrical model consists of 27 generations and $C_{27}^{(3)}$ is exemplified; (b) $k=6$. The 6CF geometrical model consists of 40 generations and $C_{40}^{(6)}$ is exemplified; (c) $k=100$. The 100CF geometrical model consists of 250 generations and $C_{250}^{(100)}$ is exemplified.

support of the measure is covered with boxes of size ε and $p_i(\varepsilon)$ is denoted as the probability (integrated measure) in the i th box, an exponent (singularity strength) α_i can be defined as

$$p_i(\varepsilon) \sim \varepsilon^{\alpha_i}. \quad (11)$$

If we count the number of boxes $N(\alpha)d\alpha$ where the probability p_i has singularity strength between α and $\alpha+d\alpha$, then $f(\alpha)$ can be loosely defined as the fractal dimension of the set of boxes with singularity strength α . That is

$$N(\alpha)d\alpha \sim \varepsilon^{-f(\alpha)}d\alpha. \quad (12)$$

The $f(\alpha)$ singularity spectrum provides a mathematically precise and naturally intuitive description set of dimension $f(\alpha)$ possessing singularity strength. On the other hand, it should be mentioned that the generalized dimension D_q provides an alternative description of the singular measure. It is defined as

$$D_q = \frac{1}{q-1} \lim_{\varepsilon \rightarrow 0} \frac{\ln \sum_i [p_i(\varepsilon)]^q}{\ln \varepsilon}. \quad (13)$$

D_q corresponds to scaling exponents for the q th moments of the measure.

In the case of diffraction spectrum, the positive quantity is the Fourier intensity, and the support is reciprocal space, i.e., the space of wave vectors Q . A straightforward application of multifractal formalism requires the evaluation of exact integral of the intensity measure of the structures with infinite length over small segment of length in the space of wave vectors. In this case, the computer time for calculation will increase incredibly. To solve this problem, an approximate scheme is chosen.²¹ Instead of calculating the infinite KCFS, we only deal with a structure which contains repeating copies of finite generation, i.e., $C_n^{(k)}$ of the original structure. It is known that Fourier transform of a periodic structure consists of Bragg peaks, and the diffraction vectors are

$$Q_i = \frac{2\pi i}{N}, \quad (14)$$

where i covers all the integers, and $N = N_n^{(k)}$ is the total number of letters in $C_n^{(k)}$. The diffraction amplitudes are

$$A_i = \frac{F_n^{(k)}(Q_i)}{N}. \quad (15)$$

Since the amplitudes of the Fourier transform $F_n^{(k)}(Q)$ shown in Eq. (6) are periodic functions of Q , we can only consider the situation in one period of reciprocal space, i.e., one Brillouin zone, and the diffraction vectors correspond to $i=1, 2, \dots, N$.

An essential ingredient in multifractal characterization is the probability weights p_i . Here, p_i is denoted as the weight of the diffraction intensities in Fourier transforms, i.e.,

$$p_i = \frac{|A_i|^2}{\sum_{i=1}^N |A_i|^2}. \quad (16)$$

The partition function can then be expressed as

$$Z(q) = \sum_{i=1}^N p_i^q,$$

$$Z'(q) = \frac{dZ}{dq} = \sum_{i=1}^N p_i^q \ln p_i, \quad (17)$$

$$Z''(q) = \frac{d^2Z}{d^2q} = \sum_{i=1}^N p_i^q (\ln p_i)^2,$$

where parameter q provides a microscope for exploring different regions of the singular measure. For $q > 1$, $Z(q)$ amplifies the more singular regions of p_i , while for $q < 1$ it accentuates the less singular regions. For $q=1$ the measure $Z(1)$ replicates the original measure. The $f(\alpha)$ curve of any finite sample is therefore available at a local level, i.e., for a given space of wave vectors Q . The values of α and $f(\alpha)$ are given by

$$\alpha = -\frac{Z'(q)}{Z(q) \ln N},$$

$$f(\alpha) = \frac{1}{\ln N} \left(\ln Z(q) - \frac{qZ'(q)}{Z(q)} \right), \quad (18)$$

and the curvature C of the $f(\alpha)$ curve at its top is

$$\frac{1}{C} = \frac{1}{\ln N} \left(\frac{Z'(0)^2}{Z(0)^2} - \frac{Z''(0)}{Z(0)} \right). \quad (19)$$

The generalized dimensions relate to the spectrum of singularity $f(\alpha)$ by Legendre transform shown below:

$$f(\alpha) = \alpha q - (q-1)D_q.$$

$$\alpha(q) = \frac{d}{dq} (q-1)D_q. \quad (20)$$

In order to check the multifractality of the Fourier intensities of the KCFS, it is essential to investigate the behavior of the curvature C of the $f(\alpha)$ curve at its top defined by Eq. (19). Figure 2(a) shows the curvature C against the generation label n for the 3CF structure. The lowest data point in the figure corresponds to $n=27$, i.e., $N_{27}^{(3)}=27$ 201 letters or atoms as shown in Table I. In the region of large n , the curvature C decreases almost linearly with a slope $s \doteq -0.036$. By the same procedure, a series of slope s can be obtained for the different KCF structures [shown in Fig. 2(b)]. Figure 2(b) indicates that for $1 < k \leq 5$ the slope of the plot of curvature C vs generation label n , i.e., s , is not equal to zero. Therefore the curvature C of the $f(\alpha)$ curve diverges as the generation number n approaches infinite. Meanwhile, the $f(\alpha)$ curve shrinks to one point, and the Fourier spectrum of the infinite chain is not a multifractal. Actually for $1 < k \leq 5$ the Fourier intensity distributions of the KCFS possess quasiperiodicity. These scale invariant structures can be characterized via a single exponent or a finite set of exponents as mentioned in Sec. II.

The situation is different in the case of the KCFS with $k > 5$. According to Eqs. (16)–(18), we got $f(\alpha)$ spectra of the KCFS for $k=6$ to 10, 20, 30, 40, 50, 80, and 100. The parameters used in the calculations are listed in Table I. An

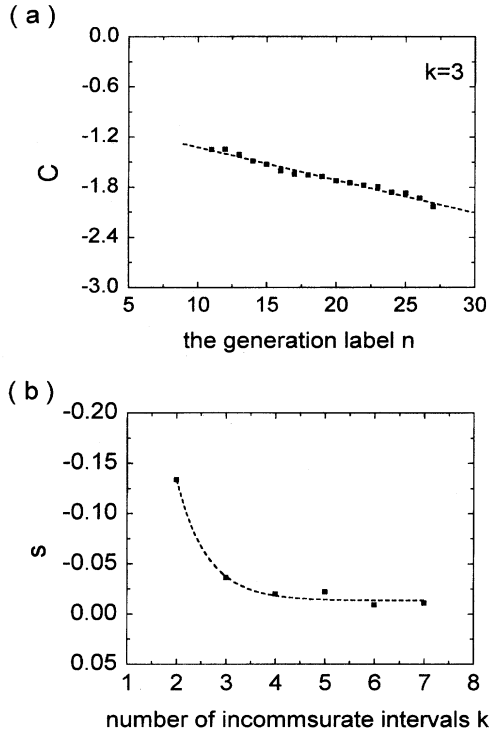


FIG. 2. (a) Plot of curvature C of $f(\alpha)$ curve of the 3CF structure against the generation label n . The slope of the dashed line is $s \doteq 0.036$. (b) Plot of the slope s vs k in the KCFS. k is the number of incommensurate intervals in the structure.

example is given in Fig. 3(a), which illustrates the $f(\alpha)$ curves of the 6CF structure and 100CF structure, respectively. From Fig. 3(a) one may find that the data points can fit perfectly into a smooth curve, which is a characteristic of an infinite structure. These $f(\alpha)$ curves can be approximately fitted by the polynomials. For instance, the $f(\alpha)$ spectrum of the 100CF structure can be formulated by $f(\alpha) = -0.9652 + 3.677\alpha - 1.973\alpha^2 + 0.2184\alpha^3$. The quantity $f(\alpha)$ is commonly the dimension of the set of wave vectors Q in the diffraction spectrum. Around each Q , the intensity measure scales as

$$|H(Q+\varepsilon) - H(Q)| \sim \varepsilon^\alpha (\varepsilon \rightarrow 0), \quad (21)$$

where $H(Q) = \lim_{n \rightarrow \infty} \int_0^Q I_n^{(k)}(Q') dQ'$, and $I_n^{(k)}$ is given by Eq. (7). It is interesting to note the physical meaning of the $f(\alpha)$ spectrum of a Fourier transform.

(i) The abscissa α_0 of the summit of $f(\alpha)$ curve, which corresponds to $q=0$, is the strength of a generic singularity. In some senses, the exponent α_0 characterizes the behavior of the intensity at a generic wave vector. Obviously $f(\alpha_0) = 1$, because the support of the Fourier transform is the whole real Q axis. Figure 3(b) shows the strength of the singularity α_0 in the KCFS. For $k > 5$, $\alpha_0 > 1$ holds, so the intensity measure of the KCFS with $k > 5$ is a genuine multifractal.

(ii) The extremes α_{\min} and α_{\max} of the abscissa of a $f(\alpha)$ curve represent the minimum and the maximum of the singularity exponent α which acts as an appropriate weight

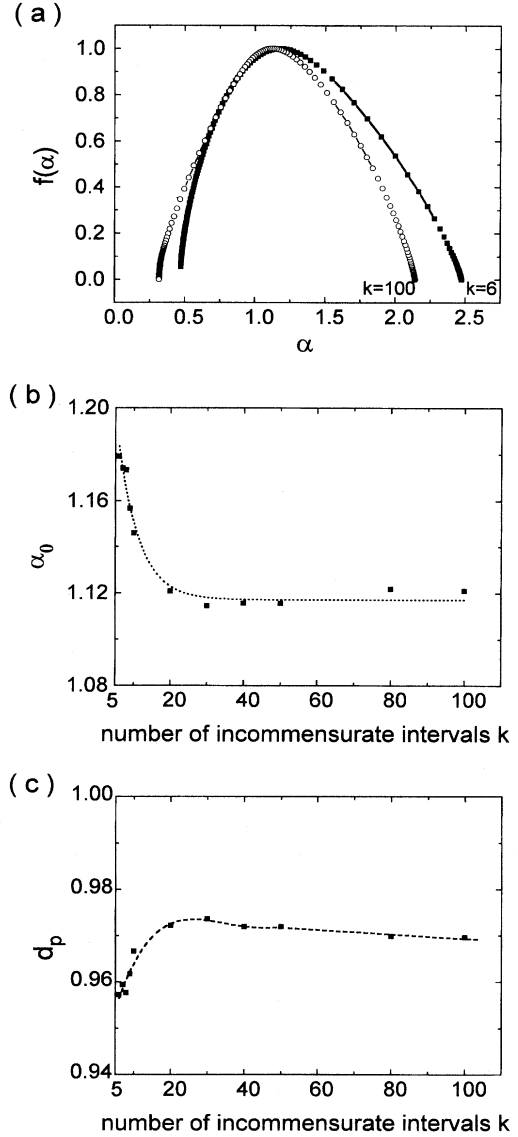


FIG. 3. (a) $f(\alpha)$ spectra of the 6CF and 100CF structures, respectively. (b) Plot of the strength of singularity α_0 in the KCFS, where k is the number of incommensurate intervals. (c) The plot to show the dimension of the set of peaks d_p in the KCFS, where k is the number of incommensurate intervals. All the dashed lines are a guide for the eyes.

in reciprocal space. In fact, $\alpha_{\min} = \lim_{q \rightarrow +\infty} D_q$ and $\alpha_{\max} = \lim_{q \rightarrow -\infty} D_q$ characterize the scaling properties of the most concentrated and most rarified region of the intensity measure respectively. With increasing of the number of incommensurate intervals k in the KCFS, the value of $\Delta\alpha = \alpha_{\max} - \alpha_{\min}$ decreases gradually [Fig. 3(a) provides the examples of $k=6$ and 100, respectively]. This implies that intensity measure of the KCFS approaches random when k increases. Actually $\Delta\alpha$ may be used as a parameter reflecting the randomness of the intensity measure.

(iii) The dimension of the set of diffraction peaks $d_p = f(1)$, corresponding to $\alpha=1$. d_p represents the dimension of the set of wave vector Q for which the local singu-

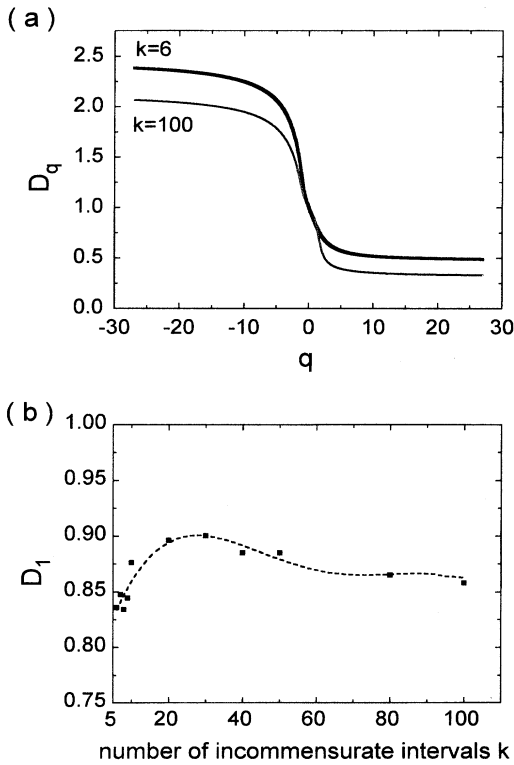


FIG. 4. (a) Plot of the generalized dimension D_q as a function of q for 6CF and 100CF structures, respectively. (b) The information dimension D_1 in the KCFS is shown in this plot, where k is the number of the incommensurate intervals in the KCFS. The dashed line is a guide for the eyes.

larity exponent α is less than unity. Figure 3(c) illustrates d_p as a function of the number of incommensurate intervals k in the KCFS. $d_p < 1$ for the KCFS with $k > 5$. When k increases, d_p increases exponentially until d_p reaches a maximum (about $d_p \approx 0.97$). Therefore, different KCFS exhibits different distribution of the diffraction peaks. When k becomes large enough, according to Fig. 3(c), we expect that the dimension of the set of peaks approaches to a constant very close to unity.

The generalized dimension D_q characterizes the nonuniformity of the measure, positive q 's accentuate the denser regions and negative q 's accentuate the rarer ones. Figure 4(a) shows the plot of generalized dimension D_q vs q for the Fourier transforms of the 6CF structure and 100CF structure, respectively. The plots of D_q vs q in Fig. 4(a) correspond to the plots of $f(\alpha)$ vs α in Fig. 3(a). It has been demonstrated that $D_q > D_{q'}$ for $q < q'$ (in the same structure). Additionally, for certain special values of q , one can take D_q as the dimension of a special set, which supports a particular part of the measure.

(i) D_0 for $q=0$, i.e., $D_0 = \lim_{\varepsilon \rightarrow 0} [\ln N(\varepsilon) / \ln(1/\varepsilon)]$, where $N(\varepsilon)$ is the number of line segments of size ε to cover the whole wave vector axis. Obviously, D_0 is the dimension of the support as mentioned above, $D_0 = f(\alpha_0) = 1$.

(ii) D_1 for $q \rightarrow 1$ is the information dimension of the intensity measure. $D_1 = \lim_{\varepsilon \rightarrow 0} [-\sum_i p_i(\varepsilon) \ln p_i(\varepsilon) / \ln(1/\varepsilon)]$, where $-p_i(\varepsilon) \ln p_i(\varepsilon)$ is an expression from information

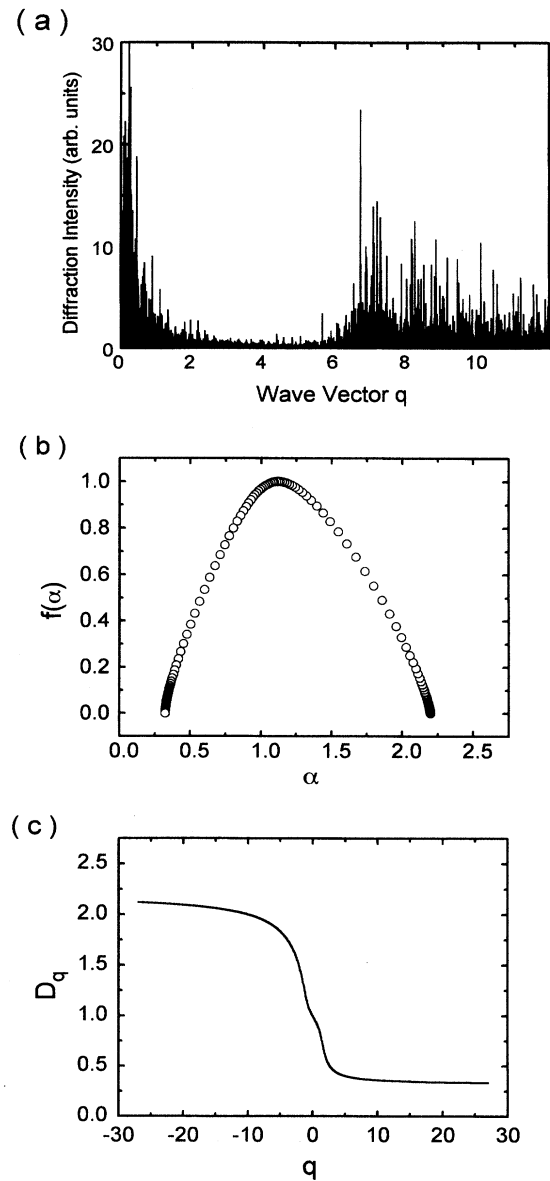


FIG. 5. (a) The Fourier transform of the 100CF structure $C_{245}^{(100)}$ which consists of 245 generations. (b) $f(\alpha)$ spectrum of the 100CF structure $C_{245}^{(100)}$. (c) Plot of the generalized dimension D_q as a function of q for the 100CF structure $C_{245}^{(100)}$.

theory and corresponds to the amount of information associated with the distribution of $p_i(\varepsilon)$ values. If the value $\alpha(1)$ is available for $q=1$, it follows that $f[\alpha(1)] = \alpha(1) = D_1$. The distance of D_1 to unity is a faithful measure of how singular the Fourier transform is. Figure 4(b) shows the information dimension D_1 in the KCFS is less than the dimension of the support D_0 , i.e., $D_1 < D_0 = 1$ for the KCFS with $k > 5$. Therefore, the intensity distribution of the KCFS with $k > 5$ is definitely a fractal measure.

(iii) D_2 for $q=2$ is the correlation dimension. $D_2 = \lim_{\varepsilon \rightarrow 0} [\ln \sum_i p_i^2(\varepsilon) / \ln \varepsilon] = \lim_{\varepsilon \rightarrow 0} [\ln \langle \mu(\varepsilon) \rangle / \ln \varepsilon]$, where $\langle \mu(\varepsilon) \rangle$ is the average density of the peaks in the wave vector interval of $\varepsilon = \Delta Q$ in the intensity measure of the KCFS. We

have $D_2(k) > D_2(k')$ in the KCFS if $k > k'$ (for example, $D_2 \approx 0.71$ for $k=6$, and $D_2 \approx 0.78$ for $k=10$). It has been demonstrated that when k becomes larger, there are more peaks occurring in the Fourier transform of the KCFS, and the diffraction spectra become more complicated.

The above analysis in reciprocal space indicates that the Fourier transforms of the KCFS possess multifractality only when $k > 5$. As k increases, these Fourier measures of the KCFS approach randomness.

Additionally, the diffraction spectrum of KCFS may contain a lot of well-defined singularities with a nonuniform background. One reason for such a behavior could be the presence in the structure of numerous motives which are more or less reproduced all the chain long. $C_n^{(k)}$ could be such a motive. One may find the difference on the diffraction spectra with different $C_n^{(k)}$. For example, the diffraction spectrum of the 100CF structure $C_{250}^{(100)}$ [shown in Fig. 1(c)] varies from the diffraction spectrum of the 100CF structure $C_{245}^{(100)}$ [Fig. 5(a)]. One may also notice their subtle difference on $f(\alpha)$ spectrum and $D_q \sim q$. For the diffraction spectrum of $C_{245}^{(100)}$, $f(\alpha)$ spectrum and $D_q \sim q$ are shown in Figs. 5(b) and 5(c). The counterparts of that of $C_{250}^{(100)}$ are shown in Fig. 3(a) and Fig. 4(a) respectively. The $f(\alpha)$ curve in Fig. 5(b) can be fitted by $f(\alpha) = -1.004 + 3.773\alpha - 2.076\alpha^2 + 0.2583\alpha^3$, which is different to that of $C_{250}^{(100)}$. Further studies on this aspect are underway.

V. CONCLUSION

One-dimensional k -component Fibonacci structures (KCFS) can be generated by defining k incommensurate intervals and ordering them in special substitution rules. The diffraction spectra of these structures are obtained from the Fourier transform of the related atomic chains. Our investigation indicates that the structure with $k=1$ is periodic, the

Fourier transform consists of Bragg peaks, which are periodically distributed in reciprocal space. In the region of $1 < k \leq 5$, the KCFS are quasiperiodic. These structures possess Pisot property and can also be generated by a projection method from k -dimensional hyperspace onto a line. Their diffraction spectra are sum of δ functions and the peaks can be indexed by a finite set of base vectors according to Eq. (10). In such a scale invariant system, the $f(\alpha)$ spectrum of the intensity measure is concentrated to a single point $\alpha = D_0 = D_q$. The KCFS with $k > 5$ are not strictly quasiperiodic. These structures usually exhibit complicated diffraction spectra. The multifractal analysis in reciprocal space reveals that these intensity measures can be characterized by a monotonic declining dependence of D_q vs q ; α distributes in a finite range $[\alpha_{\min}, \alpha_{\max}]$; $f(\alpha)$ turns to be a smooth function with a summit of $D_0 = 1$. Since the strength of singularity α_0 is greater than unity, the Fourier intensity vanishes at a generic wave vector. So the intensity measure does not have absolutely continuous component. Therefore, the Fourier transforms of the KCFS with $k > 5$ are singular continuous and possess multifractal properties. Finally, we want to emphasize that the KCFS provide a generic model which covers several types of order: periodicity, quasiperiodicity, and multifractals between quasiperiodicity and randomness. The diffraction spectra of the KCFS exhibit different characterizations of Bragg scattering of periodic and quasiperiodic structures, and the features of singular scattering of non-Pisot-property KCF structures.

ACKNOWLEDGMENTS

This research was supported by the National Natural Science Foundation of China and a grant for key research projects from the State Science and Technology Commission of China, and also the provincial Natural Science Foundation of Jiangsu.

-
- ¹B. Simon, *Adv. Appl. Math.* **3**, 463 (1982).
²M. Kohmoto, L. P. Kadanoff, and C. Tang, *Phys. Rev. Lett.* **50**, 1870 (1983).
³S. Ostlund and R. Pandit, *Phys. Rev. B* **29**, 1394 (1984).
⁴D. Levine and P. J. Steinhardt, *Phys. Rev. Lett.* **53**, 2477 (1984).
⁵R. Merlin, K. Bajema, R. Clarke, F. Y. Juang, and P. K. Bhattacharya, *Phys. Rev. Lett.* **55**, 1768 (1985).
⁶A. Hu, C. Tien, X. Li, Y. Wang, and D. Feng, *Phys. Lett. A* **119**, 313 (1986).
⁷D. Schechtman, I. Blech, D. Gratias, and J. W. Cahn, *Phys. Rev. Lett.* **53**, 1951 (1984).
⁸J. Todd, R. Merlin, and Roy Clarke, *Phys. Rev. Lett.* **57**, 1157 (1986).
⁹N. M. C. Dharma-wardma, A. H. MacDonald, D. J. Lockwood, J. M. Baribea, and D. C. Houghton, *Phys. Rev. Lett.* **58**, 1761 (1987).
¹⁰R. W. Peng, A. Hu, and S. S. Jiang, *Appl. Phys. Lett.* **59**, 2512 (1991).
¹¹R. W. Peng, A. Hu, S. S. Jiang, C. S. Zhang, and D. Feng, *Phys. Rev. B* **46**, 7816 (1992).
¹²T. C. Halsey, M. H. Jensen, L. P. Kadanoff, I. Procaccia, and B. I. Shraiman, *Phys. Rev. A* **33**, 1141 (1986).
¹³P. Meakin, A. Coniglio, H. E. Stanley, and T. Witten, *Phys. Rev. A* **34**, 3325 (1986).
¹⁴A. Hu, Z. X. Wen, S. S. Jiang, W. T. Tong, R. W. Peng, and D. Feng, *Phys. Rev. B* **48**, 829 (1993).
¹⁵C. Pisot, *Ann. Scuola Norm. Sup. Pisa* **7**, 205 (1938).
¹⁶E. Bombieri and J. E. Taylor, *Contemp. Math.* **64**, 241 (1987).
¹⁷Veit Elser, *Phys. Rev. B* **32**, 4892 (1985).
¹⁸G. Paladin and A. Vulpiani, *Phys. Rep.* **156**, 147 (1987).
¹⁹J. Feder, *Fractal* (Plenum, New York, 1988).
²⁰Ashvin Chhabra and Roderick V. Jensen, *Phys. Rev. Lett.* **62**, 1327 (1989).
²¹C. Godrèche and J. M. Luck, *J. Phys. A* **23**, 3769 (1990).